

Preparation and Electrochemical Performance of Cobalt Oxides

Xiyang Yan, Yansu Wang* and Zhiling Ma

College of Chemistry and Environmental Science, Hebei University,
Key Laboratory of Analytical Science and Technology of Hebei Province, Baoding 071002, China

Received: January 08, 2018, Accepted: October 30, 2018, Available online: January 28, 2019

Abstract: Cobalt oxides are prepared by calcining the precursor at different temperatures. The precursor is precipitated by using $\text{Co}(\text{NO}_3)_2 \cdot 6\text{H}_2\text{O}$ dissolved in $\text{NH}_3\text{-NH}_4^+$ buffer solution at $\text{pH}=9.75$. The samples are Co_3O_4 mixing with honeycomb-like morphology which proved by XRD and SEM analysis. The electrochemical results demonstrate that the best electrochemical performance of Co_3O_4 is exhibited when the calcination temperature is 450°C . When the current density increases from $1 \text{ A}\cdot\text{g}^{-1}$ to $10 \text{ A}\cdot\text{g}^{-1}$, the specific capacitance decreases from $453 \text{ F}\cdot\text{g}^{-1}$ to $249 \text{ F}\cdot\text{g}^{-1}$. After 1000 cycles charge and discharge at $1 \text{ A}\cdot\text{g}^{-1}$, up to 87% of the retention rate can be achieved, and the internal resistance of the material is less than 1Ω .

Keywords: Cobalt oxides; Calcination temperature; Electrochemical properties; Preparation

1. INTRODUCTION

Supercapacitors have been considered to be one of the most promising candidates for energy storage devices in recent years^[1,2], which can be classified into electrical double layer capacitor (EDLCs) and pseudo capacitors. Transition metal oxides^[3] are good choices for pseudo capacitors because they can charge and store more energy through the Faraday reaction. So far, various metal oxide materials such as MnO_2 ^[4], V_2O_5 ^[5], Co_3O_4 ^[6], Fe_3O_4 ^[7,8], and NiO ^[9,10] have been widely used in electrode materials. Recently, there is an increasing interest in the use of Co_3O_4 as electrode materials in pseudo capacitors due to its high theoretical capacitance and environmental friendly nature^[11]. Qiu^[12] prepared a nickel foam-supported shell-like Co_3O_4 array through the microwave hydrothermal method, and it showed an excellent specific capacitance. Zhao^[13] prepared the mesoporous Co_3O_4 material by in-situ synthesis template method, and its specific capacitance was $329 \text{ F}\cdot\text{g}^{-1}$. Through chemical precipitation and two-step heat treatment, Fan^[14] obtained a 3D Co_3O_4 powder material assembled by ultrathin nanosheet with its specific capacitance of $896 \text{ F}\cdot\text{g}^{-1}$.

In this paper, cobalt nitrate was added to a high enough concentration of $\text{NH}_3\text{-NH}_4^+$ buffer solution to obtain precursor, and followed by heat treatment. The affection of calcination temperature on the morphologies and electrochemical performance of cobalt oxides were characterized by XRD, SEM and electrochemical performance test.

2. EXPERIMENTAL

2.1. Materials

$\text{Co}(\text{NO}_3)_2 \cdot 6\text{H}_2\text{O}$ (>98.5%), ammonia (25wt%), KOH (>85wt%), NH_4NO_3 (>98%) all were analytical reagent and purchased from Tianjin Kermel Chemical Reagent Co. Ltd. The using materials and machines were all purchased from other companies such as acetylene black (Cabot Limited in Tianjin), foamed nickel collector (Kunshan Jiayisheng Electronics Co., Ltd) and polytetrafluoroethylene (Aladdin Chemistry Co., Ltd).

2.2. Samples Synthesis

A solution which 11.64 g of $\text{Co}(\text{NO}_3)_2 \cdot 6\text{H}_2\text{O}$ dissolved in 15 mL deionized water was dropwise added into the $\text{pH}=9.75$ buffer solution which mixed by 50 mL of ammonia and appropriate amount of HNO_3 . With 2h magnetic stirred continuously, the mixture color changed from orange to purple gradually with precipitating. Then 100 mL ethanol was added in order to make the solute precipitate completely. After 2h aged, the product was filtered, washed with ethanol and dried at room temperature, successively. Finally, it was heated with a ramp of $5^\circ\text{C}/\text{min}$ in the tube furnace at 350°C in the air for 3h, and this sample was labeled as sample A.

The sample B, C, D were prepared within the same procedures of sample A by changing the calcination temperature to 400°C , 450°C and 500°C , respectively.

2.3. Characterization

The phase identification of the sample was performed by a Bruker D8-advance X-ray powder diffractometer (Germany)

*To whom correspondence should be addressed: Email: 15131200232@163.com

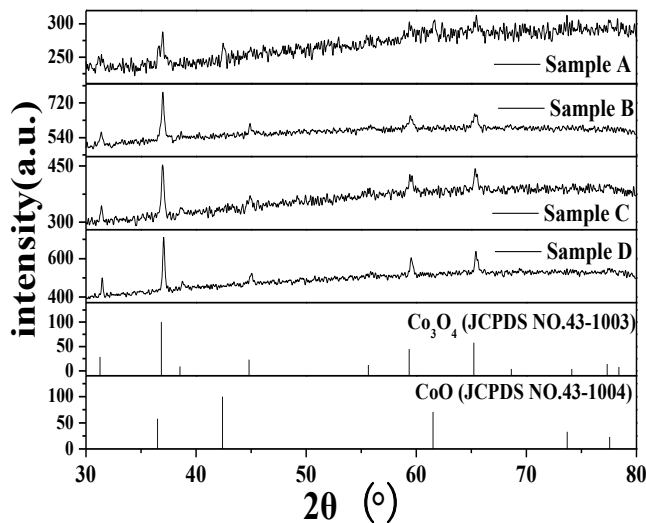


Figure 1. XRD spectrums of samples

equipped with Cu K radiation (40kV, 40mA), with a scanning speed of $10^\circ/\text{min}$. The morphology of the products were recorded on Phenom ProX Scanning electron microscopy (Holland).

2.4. Electrochemical properties

The working electrode was prepared as follows: according to the weight ratio of 80:15:5, the mixture of the cobalt oxides, acetylene black and polytetrafluoroethylene (cobalt oxides as the active material, acetylene black as the conductive agent and polytetrafluoroethylene as the binder) was pressed onto the foamed nickel collector (1cm^2) under a pressure 10 MPa, and dried at 60°C for 12 h. Prior to the test, the working electrode was immersed in a $6\text{ mol}\cdot\text{L}^{-1}$ KOH solution for 24 h at room temperature in vacuum.

Cycle voltammetry (CV), electrochemical impedance spectroscopy (EIS) (100 kHz to 0.01 Hz) and Galvanostatic charge-discharge test were performed by using GAMRY Reference1000 (USA) electrochemical workstation in a $6\text{ mol}\cdot\text{L}^{-1}$ KOH aqueous electrolyte at ambient temperature, with a standard three-electrode system containing a platinum foil counter electrode and a saturated calomel reference electrode.

According to the discharge time, the specific capacitance value of the sample was calculated as the formula: $C_s = \Delta t / m \Delta V$. Where I was the constant discharge current (A), Δt was discharge time (s), m was the cobalt oxides mass (g) of the electrode material on Ni collector, and ΔV was the potential window (V). The voltage range is 0 to 0.35V.

3. RESULTS AND DISCUSSION

3.1. Characterization of samples

XRD patterns of the samples are shown in Figure 1. The diffraction peaks at 31.4° , 36.8° , 38.5° , 44.8° , 55.7° , 59.8° and 65.1° can be respectively denoted as (220), (311), (222), (400), (422), (511) and (440) of cubic phase Co_3O_4 (JCPDS NO.43-1003). The position peaks at 36.5° , 42.4° , 61.5° , 73.7° and 77.6° in patterns belong to (111), (200), (220), (311) and (222) of cubic phase CoO (JCPDS NO.43-1004). Sample A is a mixture of CoO and Co_3O_4 while sample B, sample C and sample D are single Co_3O_4 . And the higher the calcination temperature, the better the crystallinity of Co_3O_4 is, so the crystallinity is sample D > sample C > sample B. As the temperature increases, the corresponding diffraction peak intensity of

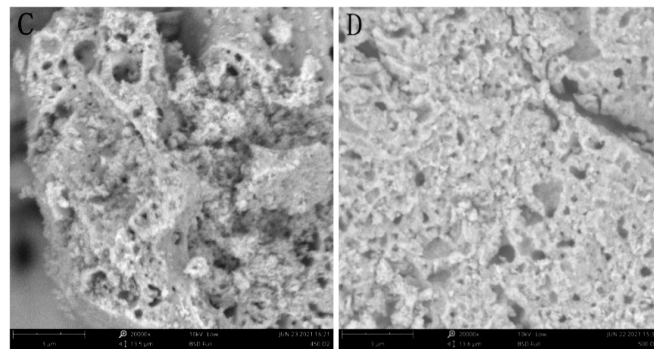


Figure 2. The SEM image of the samples

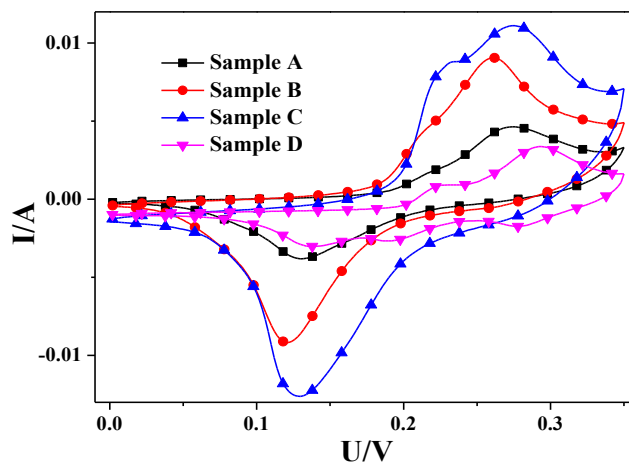


Figure 3. The cyclic voltammetry curves of the samples

the (311) crystal plane of Co_3O_4 increases and the half-width narrowed gradually. But the peak position keeps constant, which indicating that the crystal structure is stable, crystal improved and particle size increased gradually.

Figure 2 is two scanning electron micrographs of sample C and sample D at the same magnification. From the figure, samples have a honeycomb structure and the particles are stacked together irregularly. In addition, sample C has the best dispersion. But sample D was adhered each other to reduce the dispersibility of the particles. It indicates that the high heat treatment temperature is detrimental to the dispersion of the sample, and adhesion occur between particles, which may affect its chemical properties.

3.2. Electrochemical properties of the samples

Figure 3 shows a comparison of the cyclic voltammetry (CV) curves between different samples at a scan rate of $5\text{ mV}\cdot\text{s}^{-1}$. It can be seen that the samples have similar CV patterns and the positions of the redox peaks are also similar, which indicates that the same redox reactions occur during the cyclic voltammetry. The largest area covered by the curve of sample C indicates its maximal energy storage ability. The two pairs of typical redox peaks correspond to the electrochemical reaction of Co_3O_4 , which is similar to the literature data [15]. The two pairs of peaks corresponding to the mutual conversion between different oxidized cobalt [16] are as follows:

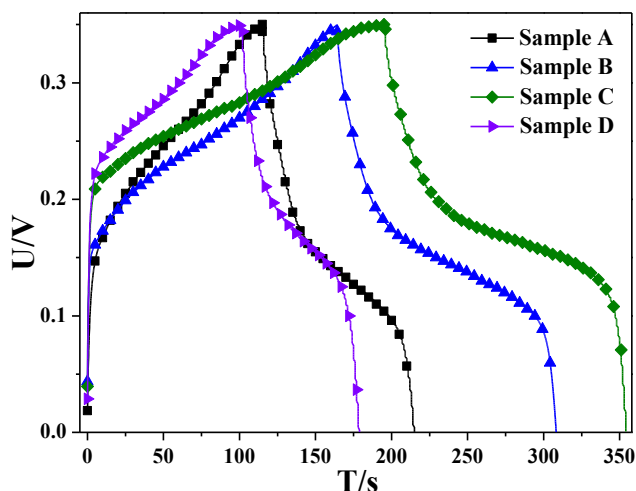


Figure 4. Charge and discharge curves for the samples at $1\text{A}\cdot\text{g}^{-1}$ current density

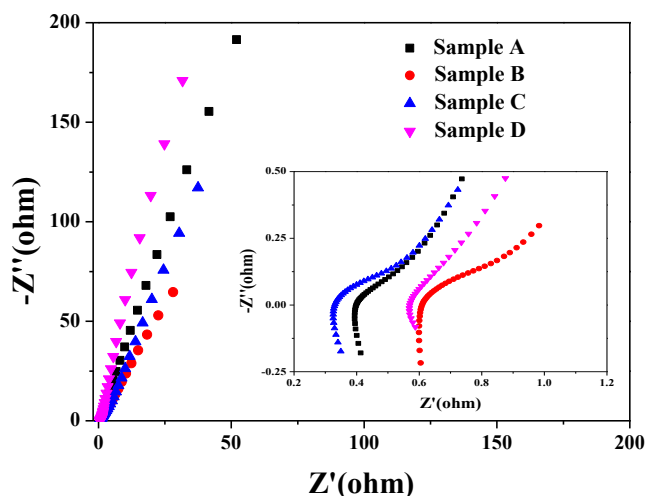


Figure 5. The EIS spectrum of samples



Figure 4 illustrates the galvanostatic charge-discharge of the samples at a current density of $1\text{A}\cdot\text{g}^{-1}$. One couple of obvious charge and discharge plateaus of curves indicate typical pseudo capacitance behavior of samples. The discharge time is sample C > sample B > sample A > sample D. By the formula in the 2.4, the longer discharge time, the higher capacitance value. So the specific capacitances are sample C > sample B > sample A > sample D. This is consistent with the cyclic voltammetry test results. The

Table 1. The specific capacitances of the samples

Sample	A	B	C	D
Specific capacitance ($\text{F}\cdot\text{g}^{-1}$)	284.03	411.43	453.71	219.26

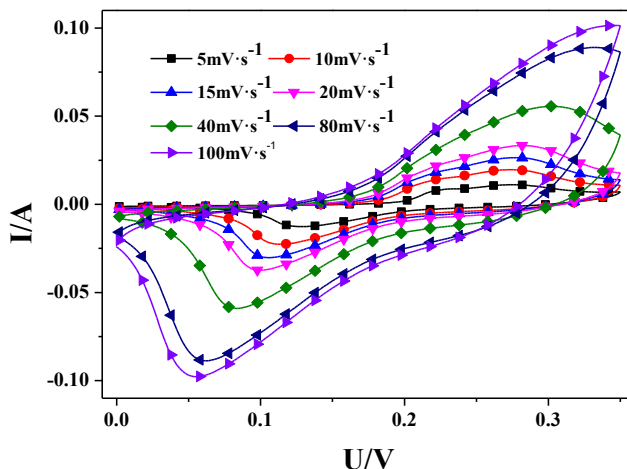


Figure 6. The cyclic voltammetry curves for sample C at different scan rates

specific capacitances of the samples are shown in Table 1.

Electrochemical impedance spectroscopies (EIS) analysis was performed and the corresponding Nyquist plots are shown in Figure 5. The illustration of Figure 5 is an enlarged view of the high frequency area. It shows that the Nyquist plots are in the form of an arc in the high frequency region and a sloped line in the low frequency region. The arc is associated with the interfacial properties of the electrodes and corresponds to the charge transfer resistance. The internal resistance is the intercept of the horizontal axis. As can be seen from the Figure 5, the internal resistances of all samples are less than 1Ω , and sample C has the smallest internal resistance, which also shows that sample C has excellent conductivity.

Figure 6 shows the CV curves of sample C at various scanning rates of 5, 10, 15, 20, 40, 80, $100\text{mV}\cdot\text{s}^{-1}$, and it indicates that the reversibility of the sample C is excellent. Due to the internal resistance of the electrode material itself and the internal resistance between the solution and the electrode, with the sweep rate increasing, the intensity of the redox peak in the cyclic voltammetry curve is gradually weakened in the three electrode system. And the corresponding oxidation and reduction peaks move toward the high voltage and low voltage, respectively^[17]. This is attributed to the effect of polarization of the electrodes. With the increase of scanning speed, the corresponding current become larger and larger, which indicates that the Co_3O_4 material has a good power performance.

A series of galvanostatic charge-discharge measurements of sample C were performed which shown in Figure 7. With current density increasing, the specific capacitance is attenuated. When the current density is large, the redox reaction on the electrode active material is not complete. When the current density increases from $1\text{A}\cdot\text{g}^{-1}$ to $10\text{A}\cdot\text{g}^{-1}$, the specific capacitance decreases from $453.71\text{F}\cdot\text{g}^{-1}$ to $230\text{F}\cdot\text{g}^{-1}$ and the capacitance retention rate is 51%, demonstrating its excellent rate capability.

The cycling stability of sample C by repeating charging-discharging processes at the current density of $1\text{A}\cdot\text{g}^{-1}$ was presented in Figure 8. From the figure, after 1000 cycles, the specific capacitance from $485\text{F}\cdot\text{g}^{-1}$ reduced to $420\text{F}\cdot\text{g}^{-1}$ and there were still 87% remaining. The experimental results show that the honeycomb Co_3O_4 electrode has a good cycle stability and has the potential to be a super capacitor electrode material.

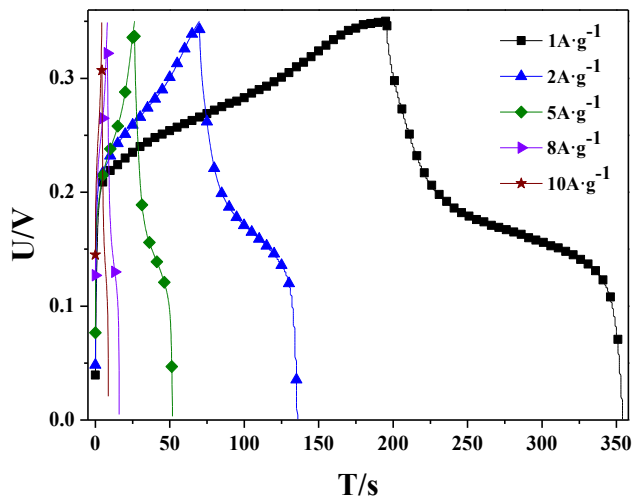


Figure 7. Charge and discharge curves of sample C at different current densities

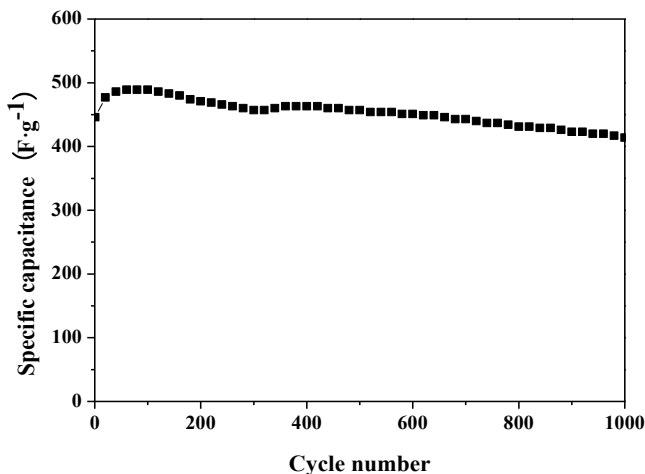


Figure 8. The specific capacitance chart of sample C

4. CONCLUSION

The honeycomb-like cobalt oxides materials were prepared at pH=9.75 for 2 hours and then calcined for 3 hours under 350°C, 400°C, 450°C, and 500°C in the air. All the results indicate that the sample C has the best electrochemical performance. When the current density increases from 1 A·g⁻¹ to 10 A·g⁻¹, the specific capacitance decreases from 453 F·g⁻¹ to 249 F·g⁻¹ with the capacitance retention rate of 51%. After 1000 cycles charge and discharge at 1A·g⁻¹, the retention rate is as high as 87%. And the internal resistance of the material is less than 1Ω. It indicates that the sample has good electrochemical performance and structural stability. Therefore, the prepared cobalt oxide materials has a good application prospect in the supercapacitor electrodes.

5. REFERENCES

- [1] Q.Q. Ke, C.H. Tang, Z.C. Yang, M.R. Zheng, L. Mao, H.J. Liu, J. Wang, *Electrochimica Acta*, 163 (2015).
- [2] M. Kumar, A.Subramania, K. Balakrishnan, *Electrochimica Acta*, 149 (2014).
- [3] C.W. Cheng, H.J. Fan, *Nano Today*, 7, 4 (2012).
- [4] J. Kang, A. Hirata, L.J. Kang, X.M. Zhang, Y.Hou, L.Y. Chen, C. Li, T. Fujita, K. Akagi, M.W. Chen, *Angew. Chem. Int. Ed.*, 52, 6 (2013).
- [5] S. Kuwabata, S. Masui, H. Tomiyori, H. Yoneyama, *Electrochim. Acta*, 46, 1 (2000).
- [6] Y.H. Xiao, S.J. Liu, F. Li, A.Q. Zhang, J.H. Zhao, S.M. Fang, D.Z. Jia, *Adv. Funct. Mater.*, 22, 19 (2012).
- [7] J.B. Mu, B. Chen, Z.C. Guo, M.Y. Zhang, Z.Y. Zhang, P. Zhang, C.L. Shao, Y.C. Liu, *Nanoscale*, 3, 12 (2011).
- [8] D.Q. Liu, X. Wang, X.B. Wang, W. Tian, J.W. Liu, C.Y. Zhi, D.Y. He, Y. Bando, D. Golberg, *J. Mater. Chem. A.*, 1, 6 (2013).
- [9] X.J. Zhang, W.H. Shi, J.X. Zhu, W.Y. Zhao, J. Ma, S. Mhaisalkar, T.L. Maria, Y.H. Yang, H. Zhang, H.H. Hng, Q.Y. Yan, *Nano Res.* 3, 9 (2010).
- [10] S.I. Kim, J.S. Lee, H.J. Ahn, H.K. Song, J.H. Jang, *ACS Appl. Mater. Interfaces.*, 5, 5 (2013).
- [11] J.H. Kwak, Y.W. Lee, J.H. Bang, *Materials Letters*, 110 (2013).
- [12] K.W. Qiu, H.L. Yan, D.Y. Zhang, Y. Lu, J.B. Cheng, W.Q. Zhao, C.L. Wang, Y.H. Zhang, X.M. Liu, C.W. Cheng, Y.S. Luo, *Electrochimica Acta*, 141 (2014).
- [13] J.C. Zhao, P. Liu, W.W. Zhang, H.J. Tangbo, J.L. Xu, *Journal of Shanghai University of Engineering Science*, 24, 3 (2010).
- [14] Y.Q. Fan, G.J. Shao, Z.P. Ma, G.L. Wang, H.B. Shao, S. Yan, *Particle Systems Characterization*, 31, 10 (2014).
- [15] J. Kang, A. Hirata, L.J. Kang, X.M. Zhang, Y. Hou, L.Y. Chen, C. Li, T. Fujita, K. Akagi, M.W. Chen, *Angew. Chem. Int. Ed.*, 52, 6 (2013).
- [16] Z.N. Yu, B. Duong, D. Abbitt, J. Thomas, *Adv. Mater.*, 25, 24 (2013).
- [17] J. Yan, T. Wei, W.M. Qiao, B. Shao, Q.K. Zhao, L.J. Zhang, Z. J. Fan. *Electrochimica Acta.*, 55, 23 (2010).